Journal of Thermal Analysis, Vol. 42 (1994) 559-593

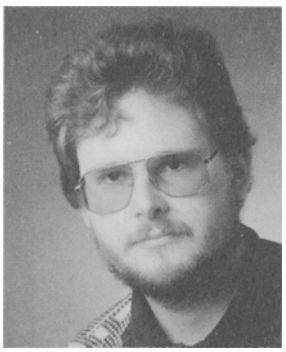

APPLICATIONS OF TEMPERATURE-RESOLVED DIFFRACTION METHODS IN THERMAL ANALYSIS

M. Epple

Institute of Inorganic and Applied Chemistry, Martin-Luther-King-Platz 6, University of Hamburg, D-20146, Hamburg, Germany

Abstract

Fundamentals and fields of application of time- and temperature-resolved diffraction methods are presented. X-ray diffraction and neutron diffraction will be considered. Dynamic diffraction methods are increasingly applied in different fields like solid state reactions, heterogeneous catalysis and biological sciences. New methods like synchrotron radiation and position-sensitive detectors permit a considerable expansion of potential research areas. The dynamic diffraction methods are compared with the classical thermoanalytical methods thermogravimetry and DSC.

Keywords: solid state reactions, time- and temperature-resolved diffraction methods, X-ray diffraction

Introduction

Reactions involving solids, i.e., heterogenous reactions, are of great importance in industrial processes. Major fields of application include areas like the roasting of sulphidic ores, decomposition reactions (e.g., burning of $CaCO_3$), synthesis of ceramics from powders and heterogeneously catalyzed reactions. More sophisticated applications include the investigation of corrosion processes, optical and magnetic data storage and the stability of drugs and other compounds in tablets.

For most of these processes thermodynamics as well as kinetics are important. While thermodynamics yield a general statement whether a process can

0368–4466/94/ $ 4.00

John Wiley & Sons, Limited
Chichester

take place at all, it does not say how fast an allowed process will proceed. However, for optimization of classical processes concerning selectivity, economy and pollution control as well as for the development of new processes, it is of major importance to gain knowledge about the different rates of the involved reactions. Consequently, chemical reaction kinetics were developed early to quantify reaction rates.

What is generally needed for a comprehensive description of a reaction is the knowledge of the amounts of substance of all reactants present in a reaction mixture at all times. Many experimental techniques are capable of yielding quantitative information for reaction mixtures and have therefore been employed in chemical kinetics. In thermal analysis, the most frequently used techniques are thermogravimetry (TG) and differential scanning calorimetry (DSC). Their main advantages are fast measurements over a temperature range with constant heating rate and small required samples sizes. For suitable reactions, the reaction extent can be computed from the parameters mass change and enthalpy change, respectively. As most solid state reactions include changes in these parameters, many of them can – at least in principle – be studied with these techniques. This has led to extensive investigations of reaction kinetics, which comprise a good part of the thermal analysis literature [1–3].

Unfortunately, reactions involving solid phases can usually not be comprehensively described in terms of a reaction extent derived from mass change and enthalpy change. New aspects that are rarely of importance for reactions in fluid (homogeneous) phases become significant for solid state reactions, and often dominate the reaction rate. They comprise inter alia nucleation effects, diffusion processes, heat conduction processes, macroscopic factors like particle size distribution and particle shape and crystal defects [4, 5]. Often the complexity of a solid state reaction is ignored, a fact that has spurred serious criticism of the classical approach to solid state phenomena [6–8].

Another important phenomenon is the occurrence of different polymorphic phases for the same chemical substance, which is due to different packing of the molecules in the crystal. A good example is carbon, which can be obtained as graphite, as diamond, or in its 'third modification' C_{60} (Fullerenes). The three forms of carbon have different physical and chemical properties, and consequently behave differently concerning reactivity. Under suitable circumstances, a polymorphic phase can transform into another phase. Amorphous phases can recrystallize. Clearly, when studying kinetics, it is very important to know which phase of each reactant is present during the course of a reaction.

Usually it is difficult or impossible to conclude from TG or DSC data alone which polymorphic phases are formed during a reaction. An examination of educts, products or quenched samples with static methods like chemical analysis of diffraction methods also does not necessarily yield the desired informa-

tion. It is therefore highly desirable to gain more insight into the reaction process, i.e., to have a more specific *in situ* method.

Suitable methods for solid state processes are diffraction methods. Their basis is the scattering of incident waves on regular crystal lattices. This is very characteristic for the investigated solid, because it is the crystal structure that determines the scattering behavior. Polymorphic phases are, of course, different regarding their structure. Contrary to TG and DSC, this method does not rely on difference information like TG (mass change) and DSC (enthalpy change). A sample can be fully characterized with a single diffractogram. Furthermore, the differences between single diffractograms can be evaluated to provide quantitative information on dynamic processes, like solid state reactions.

Diffraction methods are usually non-destructive and have become much faster in the last years because of the availability of brighter radiation sources and faster detectors. This has allowed the application of this technique as a dynamic method, i.e., in the time- and/or temperature-resolved examination of chemical processes. The method thereby fits into the definition of a thermal analysis method established by the International Confederation of Thermal Analysis (ICTAC) [9]. Some investigators successfully combined X-ray diffraction with conventional thermoanalytical methods like DTA, DSC and TG.

The mentioned new developments have led to an increasing number of applications in different fields in the last 10–15 years. Investigations were performed inter alia on solid state reactions and phase transformations, in heterogeneous catalysis, on liquid crystals, on polymers and on organized biological materials. It is the aim of this article to demonstrate the broad scope of applicability of time- and temperature-resolved diffraction methods. After reviewing the fundamentals of temperature-resolved diffraction methods, selected instructive applications will be presented to illustrate this powerful method. Although it is not a diffraction technique, a section about dynamic X-ray absorption spectroscopy is included, a method capable of examining disordered samples.

Fundamentals of diffractometry

When an electromagnetic wave falls on an ordered crystal lattice, it will be diffracted according to scattering rules. In fact, every single atom in the lattice scatters the wave, but constructive and destructive interferences permit only discrete scattering angles for an ordered lattice. These angles depend on the respective lattice geometry, the wavelength of the incident beam and the angle between the incident beam and the crystal lattice. For monochromatic waves Bragg's equation gives the relationship between these parameters:

$$n \cdot \lambda = 2 \cdot d \cdot \sin\theta \tag{1}$$

Here λ is the incident beam wavelength, d is the distance between the given set of lattice planes, θ is the angle between the incident beam and the lattice plane and n is the order of diffraction (an integer number). The fundamentals of diffractometry and crystallography can be found in numerous textbooks (see, e.g., [10–12]) to which the interested reader is referred.

X-ray diffractometry can be performed on powdered samples as well as on single crystals. Single crystal methods yield the complete structure of a particular crystal but are time-consuming. Powder methods are generally much faster but the extractable information is limited. However, it is sufficient to permit extensive statements about structural changes and to quantify present compounds, so most time-resolved experiments are carried out with powdered samples. A further drawback of single crystal methods is the requirement for a well grown single crystal, which is sometimes not easy to fulfill.

Traditionally, X-ray tubes served as radiation sources. Unfortunately, their intensity is too low to study fast processes or weakly scattering samples (like biomaterials). Consequently, after the more intense synchrotron X-radiation was employed for scattering experiments, the number of applications increased tremendously (for reviews see [13–20]). Excellent overviews for different research areas in chemistry and biology can be found in three monographs [21–23]. Due to the limited accessibility of synchrotron light sources, most research groups (except in biological sciences) still employ X-ray tubes for time-resolved experiments, which are often sufficient for processes taking place on a time-scale of minutes.

Synchrotron radiation is emitted when charged particles (usually electrons) are accelerated to relativistic speed in a circular path. The main advantages of synchrotron radiation are its high intensity and its spectral tunability. Typically, synchrotron radiation photons come with a broad frequency spectrum, which allows one to select the wavelength according to the experimental requirements [20]. Remember that conventional X-ray tubes usually emit a broad background of bremsstrahlung with few strong X-ray peaks due to the characteristic X-radiation of the anode material (e.g., CuK_α, $\lambda = 154.18$ pm), so that the wavelength is not variable. Consequently, diffraction experiments using X-ray tubes are carried out with monochromatic X-radiation, and so are most experiments using synchrotron X-radiation. However, experiments have been carried out by diffraction of polychromatic ('white') synchrotron X-radiation, a technique known as the Laue method. This can reduce the measuring time considerably, although the interpretation of results is more difficult [24–27].

The polychromatic synchrotron X-ray spectrum is also successfully used in X-ray absorption spectroscopy (XAS) which monitors the dependence of the absorption coefficient from the wavelength over a spectral range. The evaluation of absorption spectra near absorption edges allows the determination of radial

distributions functions, i.e., important structural information. Because this method does not require a crystalline material, it is finding numerous applications in many different fields. Due to the growing importance of time- and temperature-resolved applications, X-ray absorption spectroscopy will be discussed in a separate section.

Position-sensitive detectors which were developed ca. 20 years ago are able to decrease the time per X-ray diffractogram to a 100th or a 1000th of the time needed with conventional detectors like proportional counters [28–30]. The basic principle is the simultaneous recording of scattered X-ray photons over a wide angular range. This considerably enhances the performance compared to the 'old' detectors which scanned an angular range. Besides these linear detectors, some groups also developed two-dimensional area detectors based on imaging plates [31–34]. An alternative is the use of energy-dispersive X-ray scattering, in which the detector also remains fixed, allowing a decrease in measuring time [35].

The diffraction of neutrons is increasingly used in solid state chemistry [20, 36–39]. Neutron diffraction is fundamentally different from X-ray diffraction in some aspects, which opens new experimental possibilities. Contrary to X-rays which are scattered by electrons, neutrons are scattered by atom nuclei. This leads to special applications in solid state chemistry like the localization of hydrogen atoms and discrimination between neighboring elements. The magnetic moment of neutrons results in interaction with magnetic structures; therefore this effect can be employed to investigate ordered magnetic materials. The main drawback of neutron scattering experiments is the comparatively low intensity of neutron sources which usually requires longer data acquisition times and larger sample volumes compared to X-ray diffraction. However, the fact that many materials only weakly absorb neutrons facilitates the construction of heatable sample holders for time- and temperature-resolved experiments. The application of neutron and synchrotron X-ray diffraction in solid state chemistry has recently been reviewed [20].

Evaluation of diffractograms

Extensive structural and compositional information can be extracted from a diffractogram. Because most time-resolved diffraction experiments are carried out with powders, we shall demonstrate the evaluation of a powder diffractogram. With minor corrections, all considerations may also be applied to single crystal experiments. Figure 1 shows a typical diffractogram and the potentially extractable information. A powder diffractogram is usually plotted as scattering intensity *vs.* diffraction angle 2Θ.

Both intensity and position of the diffraction peaks are characteristic for the crystal structure of a given solid phase. While the peak positions depend only

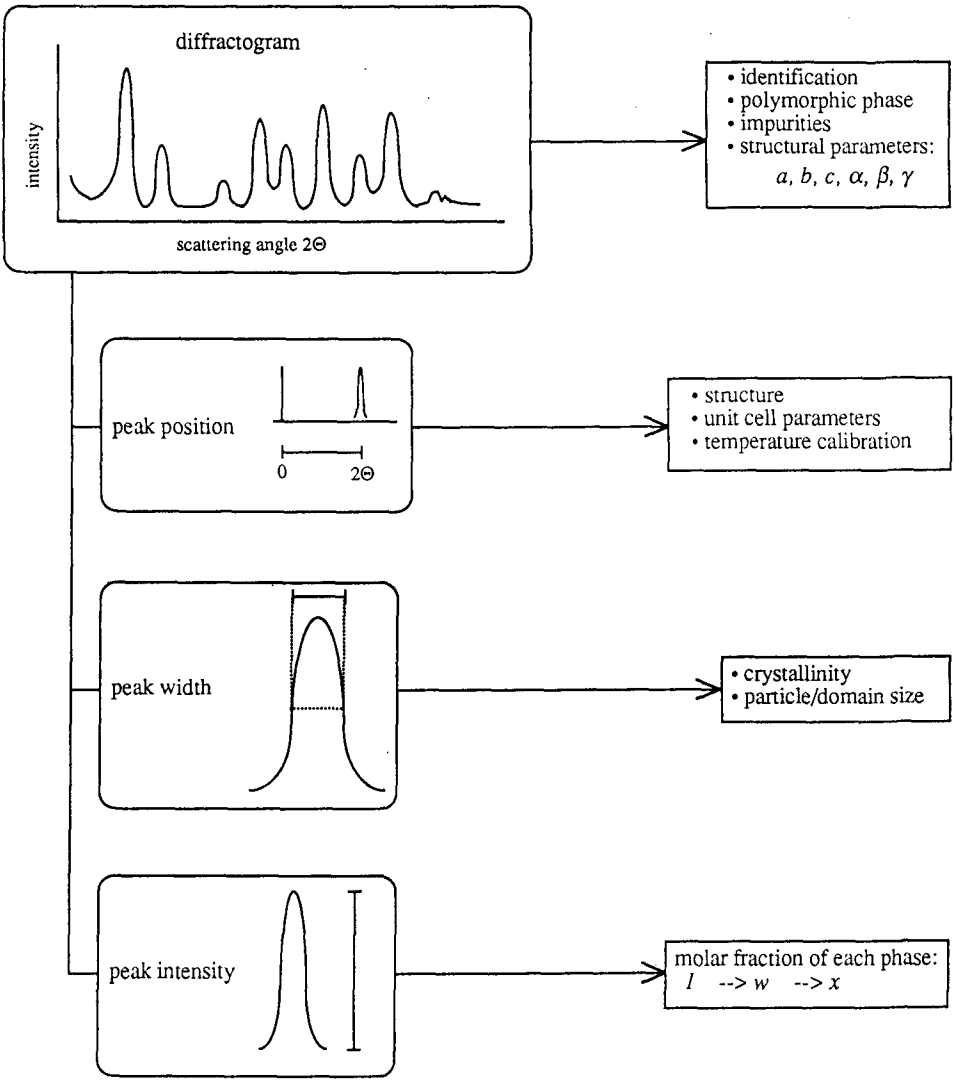

Fig. 1 The structural and compositional information extractable from a diffractogram

on the unit cell parameters (i.e., the three lengths a, b, c and the three angles α, β, γ), the relative peak intensities are determined by the positions of all atoms in the unit cell. This knowledge is often used to calculate the unit cell parameters from X-ray patterns. The Rietveld refinement method even permits determination of the positions of all atoms in the unit cell [40–42].

The uniqueness of the diffraction pattern allows the identification of a particular compound. Furthermore, as polymorphic phases have different crystal structures, they can usually be readily distinguished. If the diffractogram of the

main component is known, impurities can be detected by unassigned peaks. It shall be mentioned here that the knowledge of the six unit cell parameters alone is sufficient to calculate all possible peak positions. With that knowledge, the detection of peaks resulting from impurities is often easy.

An X-ray peak can be described by three parameters: the angular position of its maximum, its width, usually taken at the half-height (full width at half maximum, FWHM), and its height (intensity). Each of them yields specific information. As discussed, the peak position can be used to determine the structure, especially the unit cell parameters. Except for cubic crystals, more than one peak position is needed to determine the unit cell parameters. In temperature-resolved experiments, the unit cell parameters at different temperatures can be used for temperature calibration, provided that the expansion coefficient of the material is known. Discontinuities correspond to phase transitions.

The peak width depends on the crystallinity of the material [10–12]. Badly crystallized samples show broad peaks. The extreme is an amorphous phase, which may show only a very broad, flat peak. For well crystallized samples, the peak width can be used to calculate the particle or domain size. The relationship is given by the Scherrer equation:

$$D = \frac{K\lambda}{\beta\cos\theta} \tag{2}$$

with D the average crystallite size (in Å); λ the wavelength (in Å); β the peak width (FWHM, in radians); θ the diffraction angle and K a crystal shape constant near unity.

The peak width is also influenced by instrumental broadening, therefore this equation should be applied with care.

The most important parameter for solid state reactivity is the peak intensity, expressed either as peak height or peak integral. Usually there is a proportionality between these quantities, so both can be used. The peak integral is more accurate because more data points are included. However, sometimes it is difficult to determine the correct integral because of baseline uncertainties and broad peak tails. We found a good alternative by fitting an appropriate function to the peak and taking the maximum of this function as intensity value [43, 44]. This combines the advantages of including many data points and not being forced to integrate over the long tails. It also allows separation of overlapping peaks. Suitable peak functions are Gaussians, Lorentzians, Pearson functions and Voigt functions (for a comprehensive discussion see [45]). Note that the background must always be subtracted, often approximated as a linear function of the diffraction angle.

The intensity of a peak is approximately proportional to the amount of a particular phase in a mixture. To calculate the weight fraction, the different absorption coefficients for X-rays must be taken into account. The full expression for a multicomponent mixture is [10, 46].

$$I_{ij} = \frac{K_{ij} \cdot w_j}{\rho_j \cdot \mu_T^*} = K_{ij}' \frac{w_j}{\mu_T^*} \tag{3}$$

with I_{ij} the intensity of the i-th peak of component j; K_{ij} a constant characteristic for this peak; w_j the mass fraction of component j in the mixture; ρ_j the density of the pure component j; μ_T^* the mass absorption coefficient of the mixture.

We see that for those solid state reactions for which no mass change occurs, the intensity is directly proportional to the mass fraction of each compound. The composition remains constant, and so does μ_T^*. This is also true for solid-solid phase transformations.

However, during processes which involve a mass change the absorption coefficient also changes, i.e., this proportionality does not hold anymore. There are two methods to obtain the composition in these cases [10, 11, 46]. The first is to add an inert internal standard and to correct the sample reflex intensities. The second is to compute the mass absorption coefficient of the mixture by using an iterative procedure taking the reduced intensity I/I_0 as the starting value for the mass fraction [44, 47]. This procedure works as long as the mass absorption coefficient does not change too much during a reaction.

The second important thing is that the mass fraction of a compound is obtained. For kinetic evaluations usually the mole fraction is required, which means that an additional computation is necessary. To relate mass and mole fractions, assumptions are necessary about the stoichiometry of the reaction, and inert components must be known.

Not all authors pay attention to these two corrections, i.e., often a direct proportionality between reduced intensity and mole fraction is assumed. This is only true for the case of a monomolecular reaction of the type A→B without intermediates and without mass loss, e.g., a molecular rearrangement or a solid-solid phase transformation. The necessary steps for the two corrections can be found in [44].

A last correction must be applied in temperature-resolved experiments, i.e., when the sample temperature is not constant during the experiment but raised or lowered with a constant rate. In this case a possible temperature dependence of the constant K_{ij} must be taken into account. It is usually only small for limited temperature intervals (ca.100 K), but can lead to some distortions in the α/T-curve. The best way to include this variation is to determine peak intensity variations of the reaction product in a subsequent run and correct the initial val-

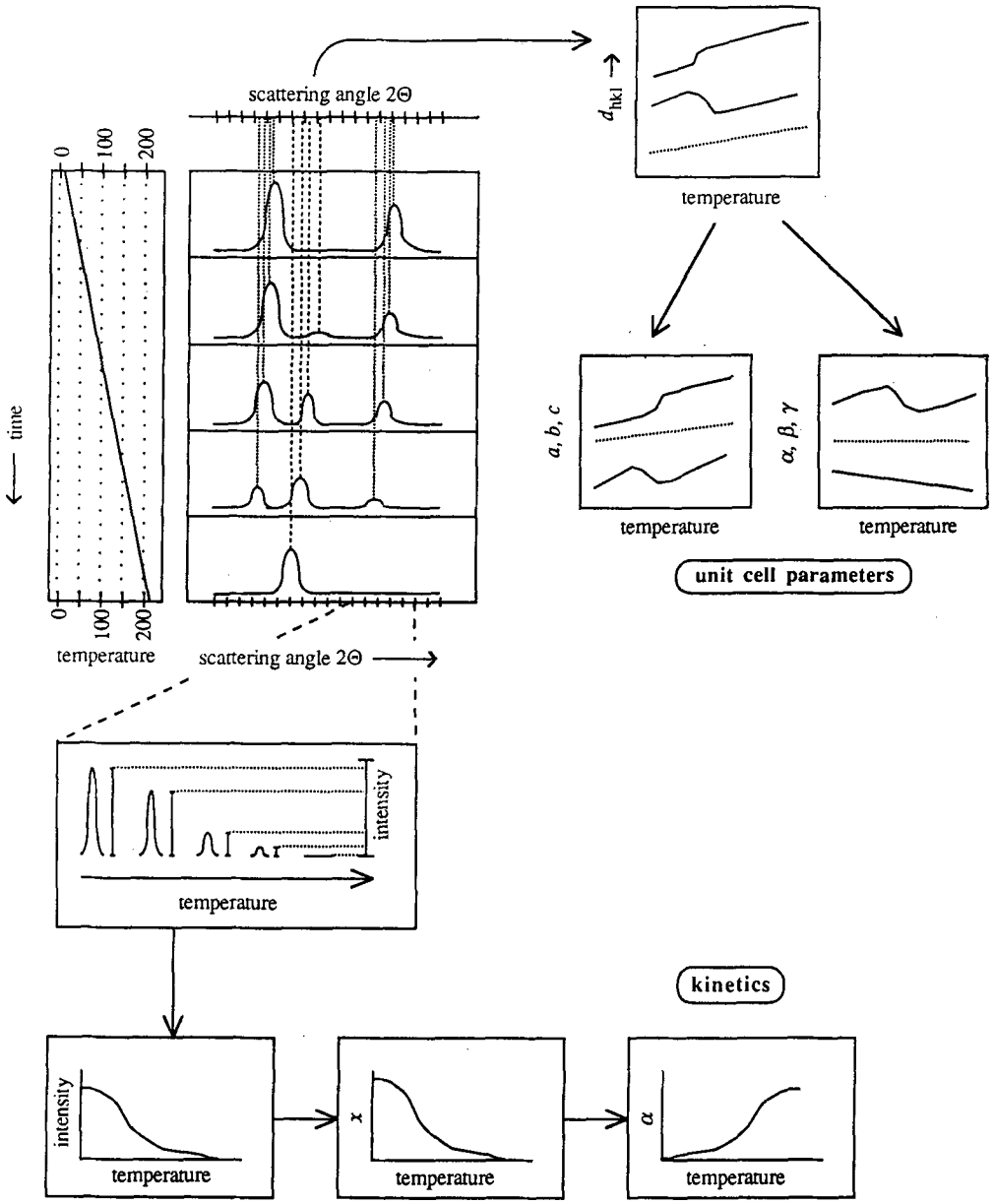

Fig. 2 Evaluation of a temperature-resolved diffraction experiment. Both structural (top and right) as well as kinetic information (bottom) can be obtained. The kinetic information is also obtainable from a time-resolved experiment at constant temperature, then giving α/t-curves

ues. Educt peak intensities must be corrected by extrapolating the peak intensities of the unreacted educt (temperature interval before the reaction) to higher temperatures.

An alternative way for evaluating series of subsequent X-ray diffractograms was proposed by Engel and Eisenreich [48–50]. Here the differences between the single angular data points are computed and their absolute values are added. This reduces the huge data amount to one number per diffractogram. The evaluation is possible in a differential and an integral way, producing DSC- and TG-like curves, respectively ('difference spectra'). In favorable cases (isothermal experiments, single step reaction) the reaction extent can be directly computed from the difference spectra.

Figure 2 demonstrates how temperature-resolved experiments (here with a constant heating rate) can be evaluated. In the upper left part five diffractograms taken at different temperatures are shown. Two educt peaks decrease as the reaction proceeds, and one product peak appears. By analyzing the variation of the intensity of one peak (diagram below) one can compute the temperature-dependent mole fraction which subsequently yields the reaction extent α. The knowledge of α at different temperatures with a constant heating rate is enough to calculate the reaction kinetics. This analysis can be performed with all three

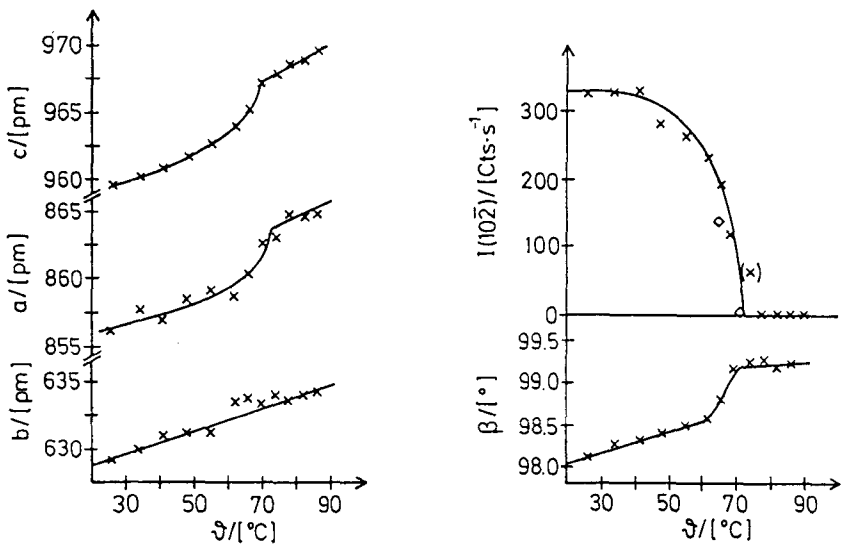

Fig. 3 Temperature dependence of the unit cell parameters of phenanthrene during a solid-solid phase transition. Both *a* and *c* exhibit discontinuities at the transition temperature of 72–74°C. The scattering in *b* is too strong to conclude safely that a discontinuity exists. The monoclinic angle β also shows a distinct step. Additionally the temperature dependence of a characteristic reflex which disappears in the high-temperature phase is shown. (From Ref. [44], with permission)

peaks, thereby tripling the database. Of course, one can also perform isothermal experiments ('time-resolved'), obtaining α-t curves.

By examining the temperature-dependent peak positions (upper scale and diagrams on the right) it is possible to obtain the corresponding d_{hkl}-values (Bragg's equation (1)). By choosing and combining suitable peaks, one gets the temperature dependence of the unit cell parameters. These gives the expansion coefficients and, more interestingly, phase transformations show up as discontinuities.

This has been demonstrated numerous times in the literature. As an example the phase transition of solid phenanthrene shall be presented. Phenanthrene undergoes an order-disorder transition at 72–74°C [44, 51, 52]. In Fig. 3 the temperature dependence of the unit cell parameters of phenanthrene is shown. Two unit cell lengths show distinct discontinuities while the scattering in the third one is too strong to make a definite conclusion. The monoclinic angle β experiences a similar step (note that the two other angles α and γ are 90°). Additionally the temperature dependence of a characteristic reflex is shown which vanishes in the high-temperature phase. From this temperature dependence the expansion coefficients can be calculated.

One of the main strengths of temperature-resolved diffraction techniques is the possibility to detect all present compounds simultaneously. As long as the compounds are crystalline, the evaluation of their corresponding peaks yields their relative amounts in the reaction mixture. This clearly distinguishes the method from 'overall methods' like DSC or thermogravimetry. Withe these it is not possible to split up a mass or enthalpy change between two or more overlapping processes.

This chapter should demonstrate the wealth of information which can be obtained from time- and temperature-resolved diffraction experiments. Figure 4 comprises the necessary steps to perform kinetic experiments. The conditions shown apply mainly to X-ray powder diffractometers, however, they can be easily adapted for other types of experiments.

Applications

Applications of time- and temperature-resolved diffraction methods are found in many fields of the physical, chemical and biological sciences. In this chapter, instructive examples will be presented to illustrate the experimental possibilities.

There is no commonly accepted abbreviation for temperature-resolved diffraction methods. Most investigators give their method a new name, usually with an 'XRD' or 'XD' (common short for X-ray diffraction) in the abbreviation. In my opinion, the form 'TXRD' is best suited, because it is close to 'XRD', and because the '*T*' immediately implies 'temperature' or 'time'.

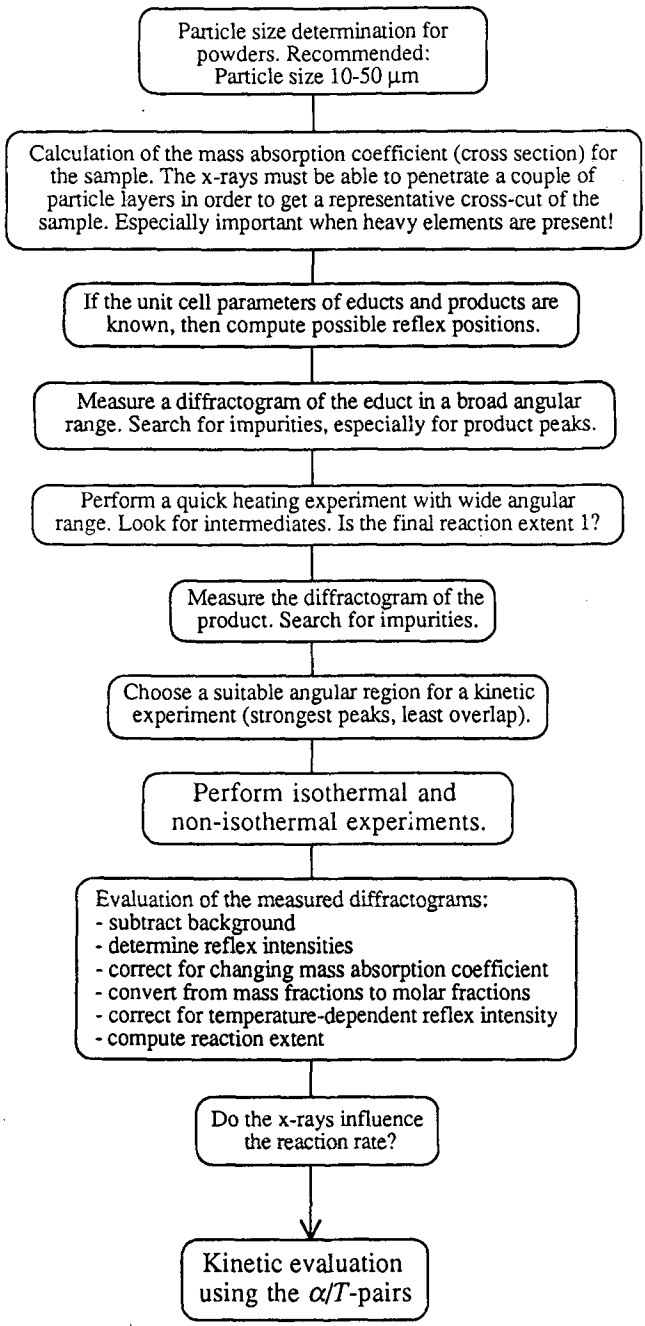

Fig. 4 The necessary steps for a kinetic experiment with temperature-resolved X-ray diffractometry. The statements are designed for powder experiments, but apply also mainly to other types of temperature-resolved diffraction experiments

Therefore this abbreviation may serve for both time- and temperature-resolved methods. In this article, 'TXRD' is used throughout, even when referring to other work, for the sake of uniformity.

Solid state reactions

Numerous methods are employed for the investigation of solid state reactions. Probably the most important techniques are structure-solving methods (single crystal diffraction, powder diffraction, solid state NMR, etc.) and thermal analysis methods (thermogravimetry, DSC, thermomechanical analysis, etc.), the first ones mainly static methods, the second ones dynamic methods.

Temperature-resolved diffraction techniques combine both kinds of methods. They allow the determination of structural information in a dynamic way. One of the first to apply this to solid state reactions was Gérard in the 1960's and 1970's [53–64]. He constructed heatable sample holders for X-ray diffractometry and combined the method with DTA and thermogravimetry. An example is shown in Fig. 5.

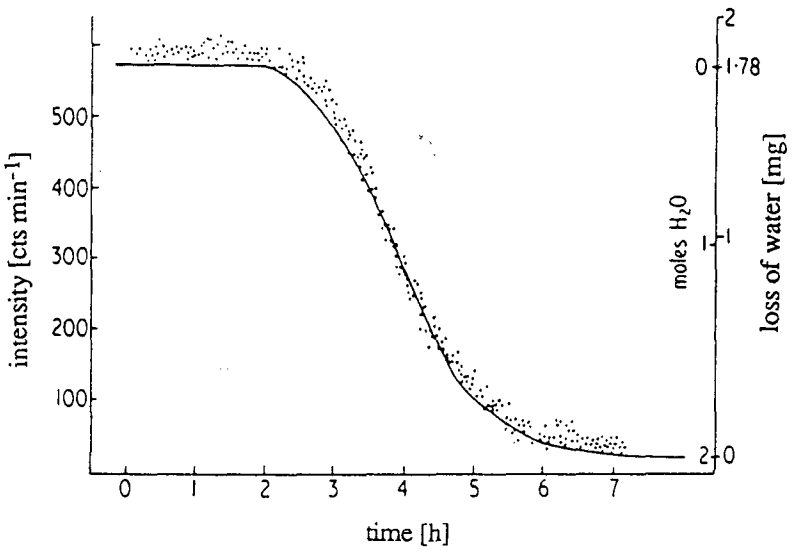

Fig. 5 The dehydration of copper sulphate trihydrate to copper sulphate monohydrate, recorded on a TG-TXRD combination. The continuous line denotes the sample mass, the dots are intensity values of a trihydrate peak (d = 4.40 Å). The dehydration was carried out at 71°C at 7 torr. (From Ref. [64], with permission)

Here the thermal dehydration of copper sulphate trihydrate to the monohydrate is studied with a TG-TXRD combination. There is complete simultaneity between the mass loss and the disappearance of an educt phase peak. This is be-

cause the mass absorption coefficient of both reactants is nearly equal, so only minor corrections apply for the intensity to reaction extent conversion. However, no quantitative evaluation of the intensity values was made, because the main aim was to check for amorphous phases during the dehydration [64].

While this was a single-step reaction with no intermediates, multicomponent reactions were investigated by Thomson *et al.* [65–67]. They examined the formation process of the 123 superconductor $YBa_2Cu_3O_{7-x}$ from an amorphous citrate precursor containing yttrium, barium and copper. The precursor was burnt prior to the experiment by holding in air for 10 minutes at 850 K. In Fig. 6 the results of the high-temperature X-ray analysis are shown. The main peaks of the reactants were recorded. When heating in helium, the 123 superconductor forms readily in a tetragonal phase (labeled 'TET 123') above 890 K. However, it decomposes at higher temperatures, forming other mixed oxides. When switching from helium to air, $BaCu_2O_2$ decomposes quickly to $BaCuO_2$, CuO, BaO and $BaCO_3$ (the latter three not shown).

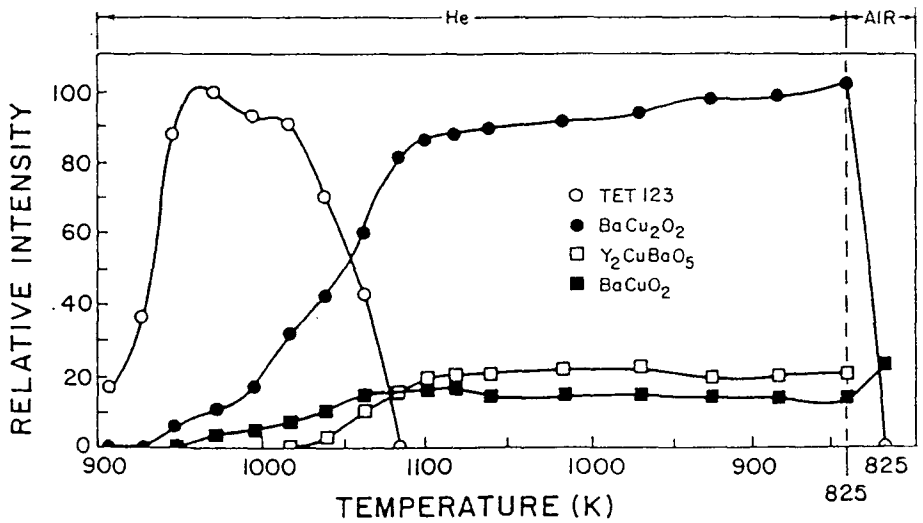

Fig. 6 Reaction sequencing during the formation of $YBa_2Cu_3O_{7-x}$ from an amorphous citrate precursor. The temperature was raised with a heating rate of 5 deg·min^{-1} from 840 to 1100 K and lowered again to 825 K. The atmosphere was then switched from helium to air, and the sample was held at 825 K for 30 minutes. 'TET 123' denotes the 123 superconductor $YBa_2Cu_3O_{7-x}$ in its fully developed tetragonal phase. (From Ref. [67], with permission. Copyright 1989 by the American Ceramic Society)

The diffraction method here not only provided detailed information about reaction products and intermediates, allowing to formulate the reaction sequences of the occurring processes, it also distinguished between the tetragonal and the orthorhombic phases of the 123 superconductor. This type of informa-

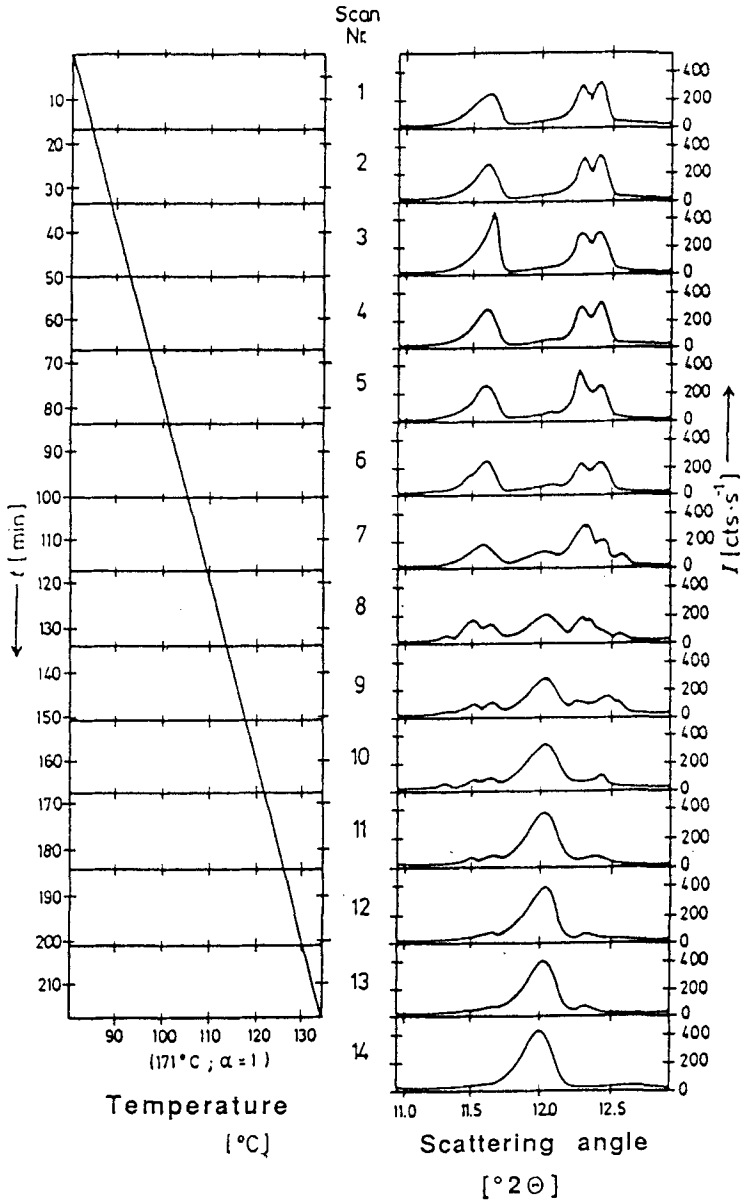

Fig. 7 TXRD scan recorded during the dehydration of silver dimesylamide quarter hydrate $AgN(SO_2CH_3)_2 \cdot 1/4H_2O$. On the left side the temperature *vs.* time is shown. The heating rate was $+0.25$ deg·min^{-1}. On the right side 14 diffractograms are shown which were recorded subsequently. Two groups of hydrate peaks disappear, and one strong anhydrate peak forms in between. Scan 14 was recorded at 171°C after the completed dehydration. (From Ref. [72], with permission)

tion would have been difficult to obtain with classical thermoanalytical methods. The classical method of annealing and rapid cooling to room temperature for X-ray investigations would also have shortcomings, as one could not exclude fast reactions taking place during the quenching step.

The quantitative evaluation of X-ray diffractograms allows the determination of the reaction kinetics, as discussed earlier. An example is shown in Fig. 7. Here 14 X-ray diffractograms are shown which were recorded during the dehydration of silver dimesylamide quarter hydrate $AgN(SO_2CH_3)_2 \cdot 1/4H_2O$. This salt is interesting as an intermediate reagent in inorganic synthesis and because it is one of the few examples of silver salt hydrates. The water is released at temperatures well above 100°C, i.e., the bonding is strong [68, 69] which is unusual for silver salt hydrates. This prompted us to determine the dehydration kinetics. A part of the X-ray diffractogram containing strong educt and product peaks was selected, and during heating with a constant rate (here: $+0.25\ \text{deg} \cdot \text{min}^{-1}$) the angular range was continuously scanned. Note that the temperature is really raised with a constant rate, not stepwise.

During the dehydration two groups of hydrate peaks are vanishing and one strong anhydrate peak is formed. A diffractogram of the pure anhydrate phase at 171°C is shown in diffractogram 14. The shrinking educt peaks showed irregular behavior, i.e., splitting (scans 6–9) or sudden, short-lived growth (scan 3). These only qualitatively reproducible effects are most likely due to a short-lived intermediate with a hydrate-like structure and to lattice distortions in the course of the dehydration. Similar effects were observed during the dehydration of lithium sulphate monohydrate [70] and the decomposition of calcium hydroxide [71]. These processes prevented a quantitative evaluation of the hydrate peaks. Nevertheless, the anhydrate peak could be used to determine the reaction extent.

Using both isothermal and non-isothermal data, the decomposition mechanism for a fine powder seems to be an initial nucleation phase, describable by an A_n mechanism, followed by a deceleratory D_3 mechanism (diffusion control). The activation energy and the preexponential factor could be calculated [72]. The values for isothermal TXRD experiments, isothermal thermogravimetric experiments and non-isothermal TXRD experiments with different heating rates agree well. It can thus be concluded that TXRD can be employed like a thermoanalytical method, i.e., experiments with a constant heating rate can be evaluated using the formalism of non-isothermal reaction kinetics [1, 73]. In this case the integral method of Kassman [74] was employed (a modification of the Coats-Redfern method).

The applicability was also demonstrated for caffeine hydrate [43, 44] and lithium sulphate monohydrate [70]. Other experiments with a kinetic evaluation of the diffraction data can be found in [35, 47, 50, 75–90].

Synchrotron radiation was necessary to investigate the solid state combustion synthesis of TiC–NiTi. In this type of reactions, a mixture of solid reactants is ignited, e.g., by an electrically heated tungsten coil or a laser. The reaction then propagates through the whole pellet within seconds, and a great amount of heat is generated, raising the temperature well above 2000°C. These fast reactions, denoted as self-propagating high temperature synthesis (SHS) or solid combustion synthesis (SCS), can be employed to synthesize ceramics, composites, etc.

Because of the rapid combustion reaction, synchrotron radiation and a position-sensitive detector had to be employed. This allowed a time resolution of 200 ms. An intimate mixture of Ti, Ni and carbon powder was pressed to a 19 mm cube. After ignition on one edge, the reaction front propagated through the pellet. A thermocouple was used to trigger the detector a few seconds before the wave front had reached the illuminated sample area. By this method the reaction at a particular area of the pellet could be conveniently observed in a time-resolved way.

The results of two combustion experiments are shown in Fig. 8. Two angular regions are scanned in two subsequent experiments. The first observations are the melting of both metals and the formation of TiC, starting at 3.4..3.6 s. At this time the wave front has reached the illuminated sample region. At 4.0 s the formation of TiC is complete. The sample now begins to cool after the completed reaction, visible by the shift of all peaks to higher 2Θ values (lattice contraction). At 13.4 s a peak of a Ti–Ni alloy appears which broadens with time. These observations allowed important insights into the steps of this fast reaction. Details on the method and further experiments can be found in [91–93].

Polymorphic phases

Many solids occur in different polymorphic phases. Their proper identification and preparation are often crucial for solid state reactivity. Solid-solid phase transformations may also occur during reactions, thereby strongly influencing the reactivity (known as the Hedvall effect). If the different phases are sufficiently stable at room temperature, an investigation may be performed with classical X-ray diffractometry on a quenched sample. However, often polymorphic phases are not stable enough, so they must be investigated *in situ*. Investigations at higher temperatures are also important for estimating the stability of pharmaceuticals which are often desired in a special polymorphic phase, frequently a metastable one.

Because there is no mass loss during a phase transition, thermogravimetry cannot be applied. DSC requires a minimum heating rate and is often not appropriate for slow processes. Furthermore, transition enthalpies are often small. TXRD requires only a structural change and can be run isothermally as well as non-isothermally and is therefore ideally suited for this kind of investigations

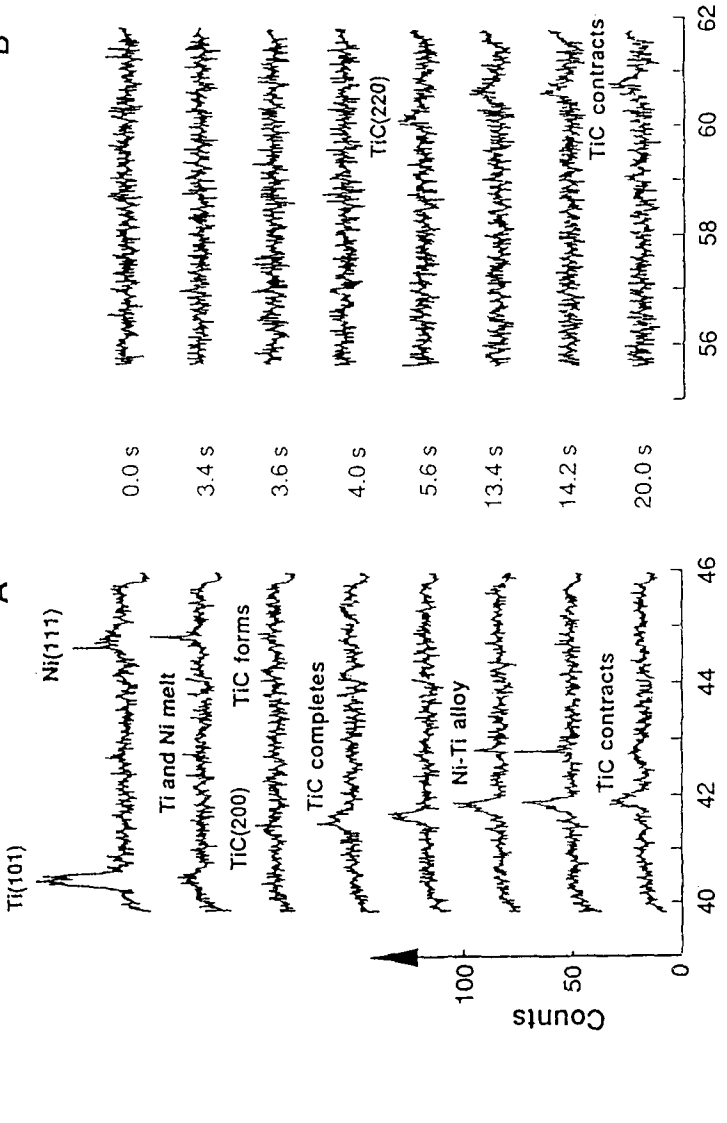

Fig. 8 The solid combustion synthesis of TiC and NiTi monitored with time-resolved synchrotron X-radiation. Two angular ranges were recorded for the reaction of titanium, nickel and amorphous carbon. At 3.4..3.6 s the combustion front reaches the illuminated area and within 0.4 s the formation of TiC is complete. After cooling, a Ni-Ti alloy forms. Note the shifting of all peaks to higher angles during the cooling, which is due to thermal lattice contraction. (From Ref. [91], with permission. Copyright 1990 by the AAAS)

[94]. No corrections are needed for absorption and weight fractions, so that the intensity directly yields the reaction extent. An application illustrates these statements. In Fig. 9 the relative amounts of low- and high-temperature phases during the phase transition in anhydrous silver dimesylamide are shown. This transition is accompanied by a very low enthalpy change which allows merely the detection of a thermal event in the temperature range of 147–153°C with DSC. No discontinuities in the expansion coefficient could be found by thermodilatometry. A detection was possible by thermoelectroconductometry with a transition temperature of 142°C. However, only TXRD allowed the quantitative evaluation of the process. It is a higher-order transformation, taking place over a wide temperature range. It is not terminated at room temperature and shows a moderate hysteresis. The signals seen in DSC and electroconductometry are obviously only the 'tip of iceberg', showing up when the transition completes near 140..150°C [72].

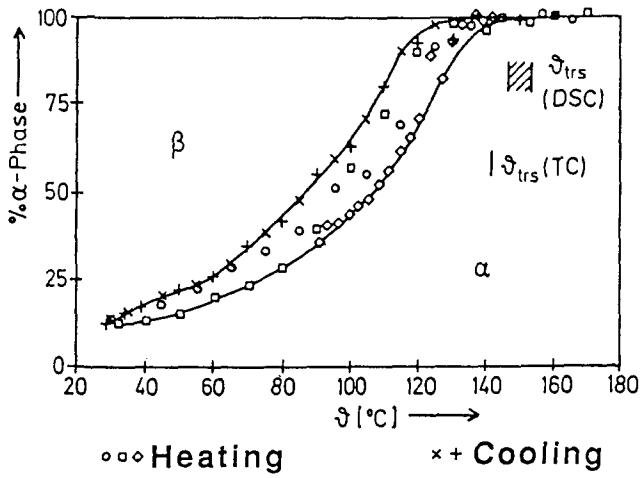

Fig. 9 X-ray investigation of the phase transition in anhydrous silver dimesylamide. From the peak intensities the relative amounts of the high- and the low-temperature phase could be computed. The low-temperature phase is denoted β, the high-temperature phase α. Both heating runs (heating rates 0.3 and 0.9 deg·min^{-1}) and cooling runs (cooling rate –0.9 deg·min^{-1}) were performed. Note the hysteresis. For comparison, the transition temperatures determined by DSC (147–153°C) and thermoelectroconductometry (EC; 142°C) are also plotted. (From Ref. [72], wit permission)

This example is typical for many cases. Often phase transitions are accompanied only by small signals in DSC: so probably many remain undiscovered. In this case, the different hygroscopicity of the two phases led us to the assumption of a phase transition. Final evidence was gained only after the TXRD experiments. It is suggested that temperature-resolved diffraction methods be

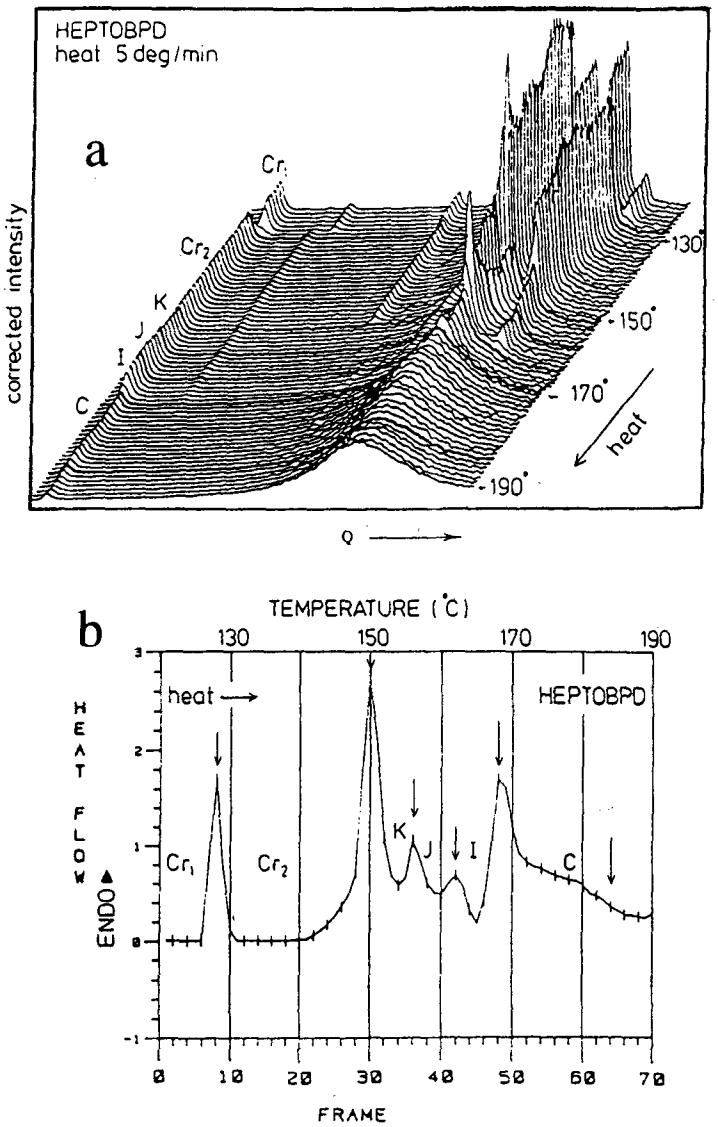

Fig. 10 Simultaneous DSC and TXRD applied to HEPTOBD (see text). The temperature range of 120–190°C was scanned with a heating rate of 5 deg·min^{-1}. **a**: The TXRD scan. Diffractograms were recorded every 12 s (1 K intervals). The X-axis variable is the wave vector $Q = (4\pi\sin\Theta)/\lambda$ with Θ the diffraction angle and λ the X-ray wavelength (154 pm). The range of *d*-spacings covered is from 3.5 Å (right) to 65 Å (left). The bold curves correspond to the arrows in the DSC curve. **b**: The DSC curve, recorded with a modified Mettler FP80/84 cell. (From Ref. [95], with permission. Copyright 1990 by Gordon and Breach, Science Publishers S.A.)

more frequently employed on solid samples showing unexplainable behavior. Phase transitions often seem not to show up with conventional techniques. Because many phase transitions do not involve drastic structure changes a close look is recommended.

Organic molecules often exhibit a number of polymorphic phases, among them frequently liquid crystalline phases. A good example of a simultaneous DSC-TXRD investigation was reported by Ungar and Feijoo [95]. They studied the phase behavior of N,N'-bis(4-*n*-heptyloxybenzal)-1,4-phenylenediamine (HEPTOBPD) with a diffractometer cell which allowed them to measure simultaneously the heat flux and the X-ray diffractogram. Synchrotron radiation was employed.

A heating scan is shown in Fig. 10. The left part of the figure shows the recorded X-ray diffractograms during a heating program from 120 to 190°C with 5 deg·min^{-1}. A number of different phases is observed: two conventional crystal phases (C_1 and C_2) and four fluid phases (crystal *K* and *J*; smectic *I* and *C*). These results compare well with the heat flux diagram, shown on the right. All phase transformations show up as endothermic peaks. Near 180°C an additional transition is observed which could not be assigned to the TXRD curve. Here it would be possible to carry out time- and temperature-resolved experiments to investigate thermodynamic (transition temperatures) and kinetic parameters (transition rate) of the numerous transitions.

Solid-gas reactions

TXRD has been successfully applied in the study of solid-gas reactions. One major application is the investigation of solid catalysts, either supported or unsupported. As still much 'art' is involved in designing efficient catalysts [96], research to understand the basic properties of a catalyst is of high importance.

Two examples will be reported. At first we discuss experiments performed by Thomas *et al.* on different catalysts with combined X-ray absorption/X-ray diffraction, operating with synchrotron radiation [97]. The long-range order (by X-ray diffractometry) and the short range order (by X-ray absorption spectroscopy, EXAFS) were obtained simultaneously. They studied the conversion of the mineral aurichalcite $Cu_{5-x}Zn_x(OH)_6(CO_3)_2$ to a mixture of ZnO and CuO during heating in air to 450°C [98]. While the crystal structure changed markedly during this process, the short range order around the copper ions and the zinc ions remained largely unchanged. This mixture was then reduced with H_2/N_2 to an active catalyst consisting of metallic copper on ZnO. Now distinct changes could be observed in the crystal structure as well as in the local environment of the copper. The zinc oxide remained unchanged. From the absorption spectra it was postulated that a small amount of zinc was incorporated in the copper structure, forming a brass phase. The authors also determined the

activity of this catalyst in the reverse water-gas shift reaction ($CO_2+H_2 \rightarrow CO+H_2O$). Further experiments with this technique were reported on mixed-metal oxides which catalyze the oxidation of carbon monoxide and hydrocarbons [99].

The reduction of iron oxide on an alumina support was studied by Jung and Thomson [87]. Iron catalysts are used widely in industrial practice, e.g., in Fischer-Tropsch synthesis, ammonia synthesis and water-gas shift reaction. Reduction experiments (with H_2) and oxidation experiments (with CO_2) were performed. During the reduction, the reaction sequence of iron(III) oxide to iron(II, III)oxide and iron metal could be monitored, and vice versa for the oxidation. An interaction between the iron catalyst and the support was found which strongly influences the catalytic performance. Other results comprise the formation of iron carbides during the Fischer–Tropsch synthesis using iron [100] and unreduced iron oxide [101]. In all cases the catalyst composition could be monitored *in situ* during the experiments. Results of other groups can be found in [102–104].

Polymers

Although polymers are generally not well crystallized, they can often be studied with diffraction methods. In Fig. 11, the melting of polyethylene is fol-

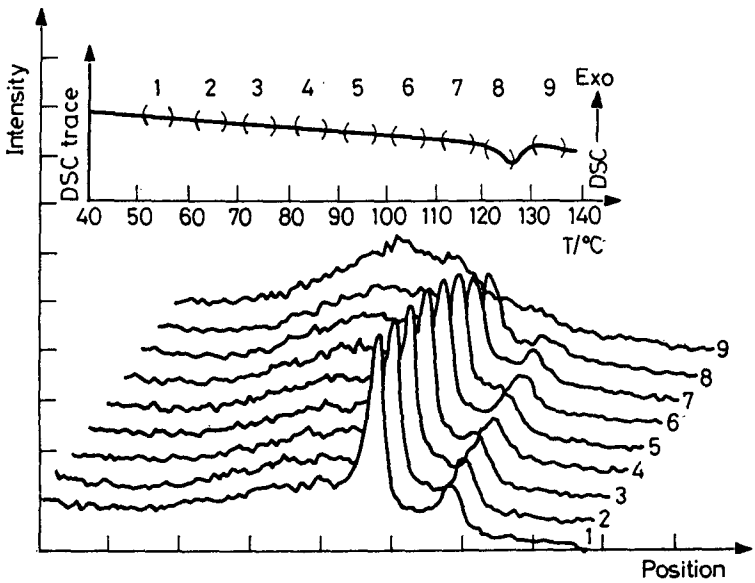

Fig. 11 The melting of polyethylene, followed with a DSC-TXRD combination. The angular range scanned was 12–32°2Θ, with one diffractogram every 5 min. The heating rate was 1.25 deg·min^{-1}. The X-ray peaks begin to shrink well below the melting temperature, which was determined to 125°C with DSC (From [105], with permission)

lowed with a DSC-TXRD combination, using a conventional X-ray source [105]. The sample was heated with 1.25 deg·min^{-1} to 140°C. Every 5 minutes an X-ray scan was recorded in the angular range of 12–32°2Θ. While the peak intensity started to decrease around 70°C in TXRD, indicating a decline in crystallinity before the melting, the DSC curve showed only a single peak at 125°C. This clearly demonstrates that premelting processes occur well below the melting temperature; a fact DSC was not able to detect. This knowledge is important, because integrated DSC peaks are often used for the determination of polymer crystallinity. Obviously, the peak integration must start below the melting point. Analogous results were obtained for the cooling process of molten polyethylene. The recrystallization persisted to lower temperatures after the solidification, invisible in DSC. Applications of synchrotron radiation on polymers are reviewed in [106]. X-ray scattering combined with DSC was also used for investigation of polymer transformations in [95, 107, 108].

Biological materials

The structural and kinetic investigation of ordered biological materials like membranes, enzymes, cell constituents, etc., is an intensively studied field in which biologists, chemists and physicists combine their efforts to gain better insight into processes occurring in living organisms. The applications of diffraction methods can be roughly divided into the investigation of lipids, i.e., long-chain organic molecules, the study of reactions of enzymes, proteins, etc., and the investigation of biological material like muscles and cell constituents. The field has been reviewed in a number of articles and monographs [21–23, 109–114] where a large number of examples can be found.

Because biomaterials are generally weak X-ray scatterers due to an imperfect crystal structure, practically all time- and/or temperature-resolved experiments are performed with synchrotron X-radiation, making use of its high intensity. In fact, researchers in biology and biophysics constitute a major part of the user group of synchrotron radiation. The applicability of TXRD shall be demonstrated in the following by using examples from the study of lipids which serve as models for biological membranes.

The many possible phases encountered in lipid systems make investigations complicated. An *in situ* investigation of phases forming at different temperatures is therefore necessary, and the time dependence of transition processes must be investigated. X-ray diffractometry is a suitable tool for phase identification, because it yields structural information. With the often employed DSC method quick information about phase changes can also be obtained; however, overlapping peaks and metastable phases make the conclusions sometimes dubious. It was also observed that the recorded thermogram depends on the thermal sample history [111, 113].

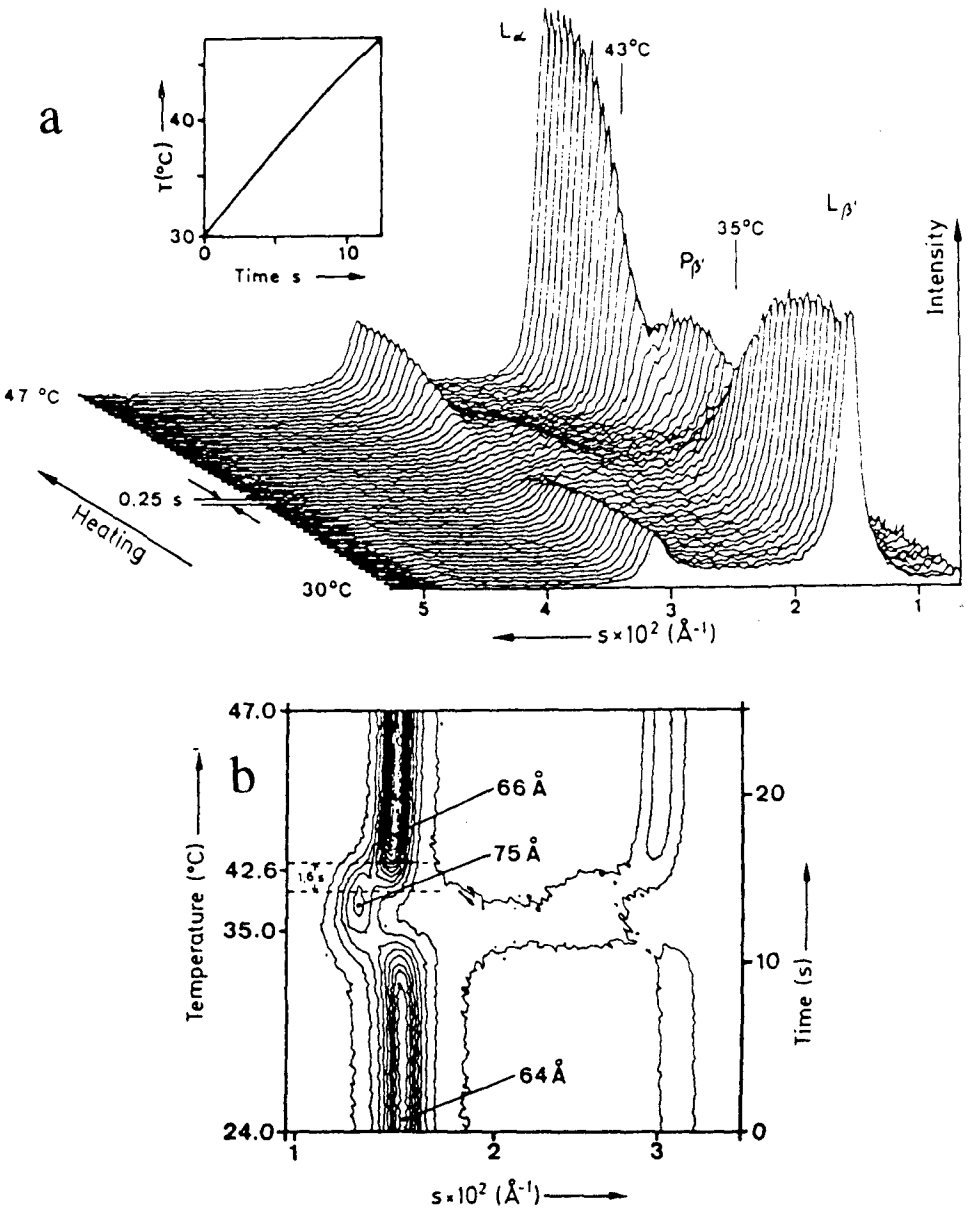

Fig. 12 Time- and temperature-resolved small angle X-ray diffraction analysis of hydrated DPPC. The sample was rapidly heated from 10 to 47°C. Synchrotron radiation was applied. The pretransition occurs around 35°C, the main transition around 43°C. The X-axis variable is $s = 1/d = 2 \sin\Theta/\lambda$; **a**: X-ray diffractograms recorded every 0.25 s in the temperature range from 30–47°C; **b**: Contour plot of the same experiment showing the temperature range from 24–47°C. (From [123], with permission)

With these facts, it is no wonder that time- and temperature-resolved diffraction techniques were applied early (beginning of the 1980's) in the study of lipid systems. Two recent examples will be presented.

Fully hydrated dipalmitoylphosphatidylcholine ('DPPC') is a standard lipid which has been extensively investigated by static [115, 116] and dynamic [117–122] methods. A temperature-resolved experiment is displayed in Fig. 12. A sample was subjected to a fast temperature jump from 10 to 47°C to study the kinetics of the phase transitions. Using synchrotron radiation and a position-sensitive detector a time resolution of 0.25 s per diffractogram was achieved. The section from 30 to 47°C is displayed in Fig. 12a in a number of diffractograms. In Fig. 12b, the data has been reduced to a two-dimensional contour plot displaying the temperature range from 24 to 47°C. Both the pretransition around 35°C and the main transition around 43°C are clearly visible. The investigators found that the transition kinetics were limited by the heat conductivity of the aqueous sample [123]. The authors reported in later publications about a laser-induced heating method capable of heating the sample in milliseconds [122, 124, 125].

A combination of TXRD and DSC was described by Chung and Caffrey [126]. Synchrotron radiation was employed in transmission mode, and modified aluminum sample holders were used in a vertically turned Mettler FP80/84 calorimeter. In Fig. 13 a set of experimental data is shown. The authors studied the L_β-to-L_α transition in monoelaidin in water which occurs around 23°C. The data were recorded with a video-based detector system and digitized after the experiment. In Fig. 13a the height of the respective (001) peak is shown, in Fig. 13b the width (half width at half maximum), in Fig. 13c the position, in Fig. 13d the computed d-spacing and in Fig. 13e the integrated peak area. Figure 13f displays the DSC curve. The discontinuities all take place in the same temperature range, nicely illustrating the phase transition. The authors found good agreement in the transition temperature ranges between DSC and TXRD for a heating rate of 1 deg·min^{-1} but report discrepancies for heating rates of 5 and 10 deg·min^{-1}. These were assigned to temperature gradients within the sample holder.

Coupling of diffractometric methods with other thermoanalytical techniques (simultaneous methods)

A number of researchers successfully coupled temperature-resolved diffractometry with other techniques like thermogravimetry and DTA/DSC. This further enhances the potential of the method, as generally with simultaneous methods: the coupled method generates more information then the sum of the individual methods.

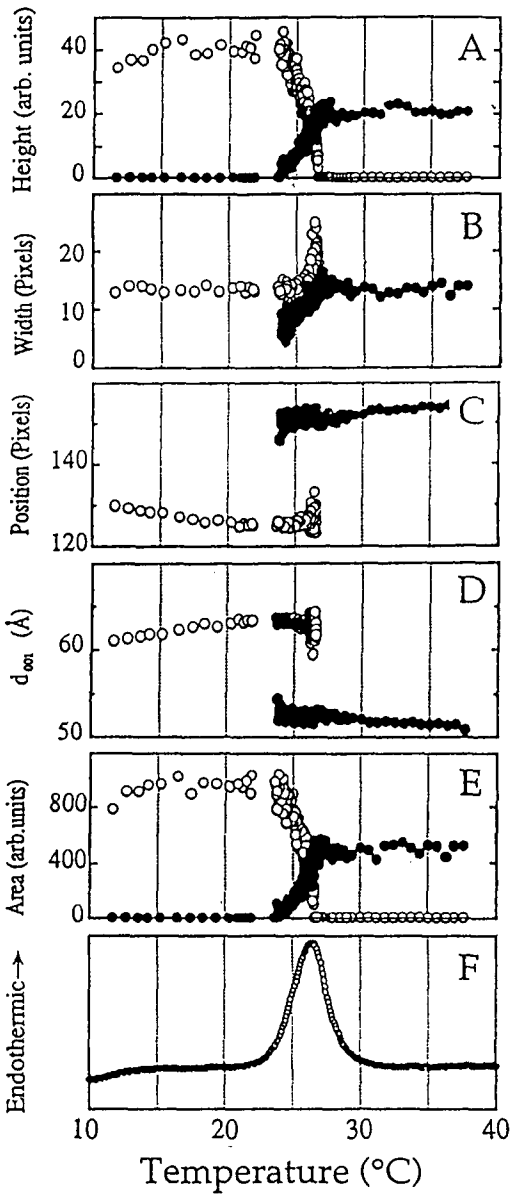

Fig. 13 Simultaneous TXRD and DSC applied to the L_β-to-L_α transition of monoelaidin in water. The heating rate was 5 deg·min^{-1}. In 13a the height of the respective (001) peak is shown, in 13b the width (half width at half maximum), in 13c the position, in 13d the computed *d* spacing and in 13e the integrated peak area. Figure 13f shows the DSC curve. (Reproduced from the Biophysical Journal, 1992, vol.63, pp.438–447, by copyright permission of the Biophysical Society [126])

In Table 1, examples of investigators are presented. The first combination methods date back to the 1960's.

Time-resolved experiments using X-ray absorption spectroscopy

Although it is not a diffraction technique, a short chapter shall be dedicated to X-ray absorption spectroscopy which has gained increasing popularity in the last years. The availability of X-ray synchrotron radiation with a broad frequency spectrum has allowed the routine use of this method today. Especially interesting are absorption spectra near absorption edges of elements present in the sample, the two methods being known as Extended X-ray Absorption Fine Structure (EXAFS) and X-ray Absorption Near Edge Structure (XANES). These two methods evaluate the specific form of the absorption sectra near absorption edges, especially oscillations in the absorption coefficient above the absorption edge. These results from scattering of the emitted photoelectron on the neighboring atoms in the lattice. A Fourier evaluation permits determination of the radial distribution functions around the particular element whose absorption edge was investigated. Because each element's adsorption edge can be examined, the method yields the radial distribution functions around each sort of atoms in a given material. No regular structure is required as in diffractometry, therefore the method ideally supplements diffractometric methods. It is possible to apply it in a time-resolved way [93, 134, 135]. Consequently, a combination of X-ray diffractometry and EXAFS was reported by Thomas *et al.* [97–99] and successfully applied to catalysts.

Time- and temperature-resolved X-ray absorption experiments were also performed by Bazin *et al.* on catalysts [136, 137] and by Fontaine *et al.* in electrochemistry [138–140], high-temperature superconductors [138, 139, 141] and solid-solid phase transformations [139, 140]. The latter group denotes its technique 'QEXAFS' for Quick-EXAFS, and reports time resolutions down to 2.7 ms per spectrum. The higher intensity of new synchrotron radiation sources will allow a further decrease in measuring time.

Conclusion

I hope to have demonstrated the wide field of application possibilities for time- and temperature-resolved diffraction methods. Rather than merely reporting a summary of our work, the aim of this article was to present examples out of different research areas where these techniques are applied to a wide variety of samples.

The availability of position-sensitive detectors with enhanced spatial and time resolutions permits one to lower the time needed to record one diffractogram when using conventional X-ray tubes. As the principal applicability of X-

Table 1 Combination of temperature-resolved X-ray diffraction methods (TXRD) with other thermoanalytical techniques. The combinations of DSC cells with X-ray diffraction are denoted differential scanning calorimetry by the researchers. However, it is not always clear whether these DSC cells really work in a quantitative mode, i.e., deserve the denotation 'DSC' instead of 'DTA'

Year	Method	Researcher	Remarks
1964	DTA-TXRD	Gérard *et al.*	Patented apparatus, controlled water vapor pressure. Applied to decomposition reactions of solids [54–56, 58–60].
1965	DTA-TXRD	Wefers	High temperature cell, up to 1600°C [127].
1967	DTA-TXRD-EC	Bessonov, Ust'yantsev and Taksis	Coupling of X-ray diffractometry, DTA and electroconductometry. Demonstrated with ceramics, up to 1500°C [128].
1967	DTA-TXRD	Ravich *et al.*	Temperature interval –180...600°C [129].
1973	TG-TXRD-EGA	Wiedemann	'Thermo molecular beam analysis' (TMBA), combined with mass spectrometry [130].
1974	TG-TXRD	Gérard	Decomposition reactions of solids [64].
1985	DSC-TXRD	Fawcett *et al.*	Patented apparatus, attached to a Guinier camera [105, 131].
1986	TG-TXRD	Andersson, Azoulay and de Pablo	Thermal decomposition of sodium sulphide pentahydrate [132, 133].
1986	DSC-TXRD	Koberstein and Russel	Small angle X-ray scattering, combined with Mettler FP80/84 cell, applied to polymers [107, 108].
1990	DSC-TXRD	Ungar and Feijoo	Synchrotron X-radiation, combined with Mettler FP80/84 cell; liquid crystals and polymers [95].
1991	EXAFS-TXRD	Thomas *et al.*	Synchrotron radiation; study of the thermal behavior of catalysts and catalyst precursors [97–99].
1992	DSC-TXRD	Chung and Caffrey	Synchrotron X-radiation, combined with Mettler FP80/84 cell; phase transitions of lipids [126].
1993	TXRD	Ryan	Synchrotron X-radiation; simulatneous small angle and wide angle X-ray scattering [149].
1993	DSC-TXRD	Bark and Zachmann	Synchrotron X-radiation, combined with Mettler FP80/84 cell; simultaneous small angle and wide angle X-ray scattering and DSC [150].

Table 2 Comparison of temperature-resolved diffraction methods and the conventional thermoanalytical methods thermogravimetry and differential scanning calorimetry

Parameter	Thermogravimetry (TG)	Differential Scanning Calorimetry (DSC)	Time- and temperature-resolved X-ray diffractometry (TXRD)*
measured quantity	mass (unspecific)	enthalpy change (very unspecific)	structure (very specific)
amount of sample needed	20–50 mg	2–10 mg	100–300 mg*
data flux	ca. 1 value/s	ca. 1 value/s	ca. 0.01–0.1 value/s*
typical heating rates	0.1–50 deg·min^{-1}	0.1–50 deg·min^{-1}	0.1–2 deg·min^{-1}*
isothermal experiments	well possible	difficult	well possible
general sensitivity	medium to high	high	medium to low*
sensitivity problems when	– little or no mass change occurs	– little or no enthalpy change occurs – heating rates are small	– little* or no structure change occurs – samples are amorphous
investigation of complex reactions (e.g., parallel, consecutive reactions)	difficult	difficult	easy
data evaluation	easy	more complex	complex
miscellaneous problems	– buoyancy effects	– calibration – deconvolution – choice of baseline	– possible influence of X-radiation on the reaction – radiation damage – preferred orientation (for powders)

* The statements given for TXRD apply to a conventional X-ray source on a powder diffractometer equipped with a proportional counter and reflect the author's experience. However, utilization of synchrotron X-radiation and position-sensitive detectors can drastically enhance the performance shown here

ray diffractometry to solid state reactions has been extensively demonstrated, this will probably lead to more research groups entering this field.

The advantages of TXRD over conventional thermoanalytical techniques are summarized in Table 2, where the performance of three techniques is compared. Even when using conventional X-ray tubes equipped with 'old fashioned' detectors (i.e., without position-sensitive detectors) the technique is well suited to study solid state processes occurring not too fast. For the lucky researchers who have access to a synchrotron radiation source, intensity is usually not a problem. Nevertheless, even brighter radiation sources and improved detectors will bring the time resolution further down into the range of milli- and microseconds. This is especially interesting for the biological sciences, where time-dependent studies on enzyme-substrate reactions, lipid phases and protein crystals could then be performed in greater detail than today.

However, more solid state chemists will probably enter the user group of synchrotrons when the number and accessibility of those facilities will have increased. Today, however, solid state chemistry still seems to be underrepresented in the time-dependent studies using synchrotron radiation. The amazing results obtained by some groups, e.g., a concentration detection down to 0.01 mol-% [13], a protein crystal structure determination in 3 s [24], crystal structure determinations on crystals with dimensions of the order of microns [25, 142, 143], nanosecond resolved X-ray diffraction on silicon crystals [144–146], sub-nanosecond X-ray diffraction on LiF [147], and dynamic diffraction experiments on lipid monolayers [148] should stimulate more researchers to apply this technique to their specific problems. The theoretical limit for time resolution lies probably at a few hundred picoseconds, the typical length of an electron bundle in the storage ring.

More combinations of TXRD with classical thermoanalytical methods appear desirable. The examples given in Table 1 show that it is possible to develop these methods, and more researchers will probably build DTA-TXRD instruments which seem to be the easiest to realize. In my impression a true, i.e., quantitative, DSC-TXRD cell still has to be build. The quantitative evaluation of TXRD and DSC curves should be very helpful in the interpretation of solid state reactions, especially in the proper assignment of structure changes to enthalpy changes.

* * *

I am grateful to M. Caffrey, C. E. Crowder, T. G. Fawcett, J. L. Feijoo, P. Laggner, W. J. Thomson, G. Ungar and J. Wong for the permission to use figures from their work. I also thank the publishers of the corresponding publications for their permission. Material was also provided by A. Fontaine, D. Louër, E. Mandelkow and J. M. Thomas for which I wish to thank them. Finally, I thank H. K. Cammenga for continual support of my work, and B. A. Snyder for carefully reading the manuscript.

References

1 E. Koch, 'Non-isothermal reaction analysis', Academic Press, London 1977.
2 W. E. Brown, D. Dollimore and A. K. Galwey, 'Reactions in the solid state', in: Comprehensive Chemical Kinetics (C. H. Bamford, C. F. H. Tipper, Eds.), vol.22, Elsevier, Amsterdam 1980.
3 J. Sesták, 'Thermophysical properties of solids', in: Comprehensive Analytical Chemistry, Vol. XII, Part D, Elsevier, Amsterdam 1984.
4 E. V. Boldyreva, React. Solids, 8 (1990) 269.
5 E. V. Boldyreva, J. Thermal Anal., 38 (1992) 89.
6 M. Maciejewski and A. Reller, Thermochim. Acta, 110 (1987) 145.
7 M. Maciejewski, J. Thermal Anal., 33 (1988) 1269.
8 M. Maciejewski, J. Thermal Anal., 38 (1992) 51.
9 J. O. Hill, 'For better thermal analysis and calorimetry', International Confederation for Thermal Analysis (ICTAC), 1991.
10 E. F. Kaelble (Ed.) 'Handbook of X-rays', McGraw Hill, 1967.
11 H. P. Klug and L. E. Alexander, 'X-ray diffraction procedures for polycrystalline and amorphous materials', Wiley-Interscience, New York 1974.
12 D. L. Bish, J. E. Post (Eds.), 'Modern powder diffraction', in: Reviews in Mineralogy (P. H. Ribbe, Ed.), Vol.20, Mineralogical Society of America, Washington DC, 1989.
13 V. V. Boldyrev, Y. A. Gaponov, N. Z. Lyakhov, A. A. Politov, B. P. Tolochko, T. P. Shaktshneider and M. A. Sheromov, Nucl. Instrum. Meth. Phys. Res. Sect. A, 261 (1987) 192.
14 M. Belakhovsky, J. Chim. Phys. Phys. Chim. Biol., 86 (1989) 1453.
15 J. F. Berar, M. Bessière and S. Lefebvre, J. Chim. Phys. Phys. Chim. Biol., 86 (1989) 1473.
16 J. Goulon, J. Chim. Phys. Phys. Chim. Biol., 86 (1989) 1427.
17 L. W. Finger, 'Synchrotron powder diffraction' in: [12], p. 309–332.
18 W. A. Basset, Annu. Rev. Earth Planet. Sci., 18 (1990) 387.
19 B. Lengeler, Adv. Mat., 2 (1990) 123.
20 A. K. Cheetham and A. P. Wilkinson, Angew. Chem., 104 (1992) 1594; Angew. Chem. Int. Ed. Engl., 31 (1992) 1557.
21 E. Mandelkow (Ed.), 'Synchrotron Radiation in Chemistry and Biology I', Topics in Current Chemistry, Vol.145, Springer, 1988.
22 E. Mandelkow (Ed.), 'Synchrotron Radiation in Chemistry and Biology II', Topics in Current Chemistry, Vol.147, Springer, 1988.
23 E. Mandelkow (Ed.), 'Synchrotron Radiation in Chemistry and Biology III', Topics in Current Chemistry, Vol.151, Springer, 1989.
24 J. Hajdu, P. A. Machin, J. W. Campbell, T. J. Greenhough, I. J. Clifton, S. Zurek, S. Gover, L. N. Johnson and M. Elder, Nature (London), 329 (1987) 178.
25 M. M. Harding, S. J. Maginn, J. W. Campbell, I. Clifton and P. Machin, Acta Crystallogr. Sect. B: Struct. Sci., 44 (1988) 142.
26 K. Moffat and J. R. Helliwell, Top. Curr. Chem., 151 (1989) 61.
27 M. M. Harding, J. Phys. Chem. Solids, 52 (1991) 1293.
28 C. Riekel, 'Applications of one-dimensional position-sensitive detectors for neutron diffraction experiments on powders and liquids' in: Position-Sensitive Detectors & Thermal Neutrons, (P. Convert, J. B. Forsyth, Eds.), London 1983, p. 267–285.
29 R. A. Newmann, P. M. Kirchhoff and T. G. Fawcett, Adv. X-ray Anal., 27 (1984) 261.
30 U. W. Arndt, J. Appl. Crystallogr., 19 (1986) 145.

31 Y. Amemiya, Y. Satow, T. Matsushita, J. Chikawa, K. Wakabayashi and J. Miyahara, Top. Curr. Chem., 147 (1988) 122.
32 Y. Amemiya, S. Kishimoto, T. Matsushita, Y. Satow and M. Ando, Rev. Sci. Instrum., 60 (1989) 1552.
33 S. M. Gruner, Rev. Sci. Instrum., 60 (1989) 1545.
34 H. Iwasaki, Y. Matsuo, K. Ohshima and S. Hashimoto, J. Appl. Crystallogr., 23 (1990) 509.
35 P. Barnes, J. Phys. Chem. Solids, 52 (1991) 1299.
36 C. Riekel, Prog. Solid State Chem., 13 (1980) 89.
37 J. Pannetier, Chem. Scr., 26A (1986) 131.
38 A. W. Hewat, Chem. Scr., 26A (1987) 119.
39 R. B. Von Dreele, 'Neutron powder diffraction' in: [12], p. 333–369.
40 H. M. Rietveld, Acta Crystallogr., 22 (1967) 151.
41 H. M. Rietveld, J. Appl. Cryst., 2 (1969) 65.
42 J. E. Post, D. L. Bish, 'Rietveld refinement of crystal structures using powder diffraction data' in: [12], p. 277–308.
43 M. Epple and H. K. Cammenga, J. Thermal Anal. 38 (1992) 619.
44 M. Epple and H. K. Cammenga, Ber. Bunsenges. Phys. Chem., 96 (1992) 1774.
45 S. A. Howard and K. D. Preston, 'Profile fitting of powder diffraction patterns' in: [12], p. 217–276.
46 R. L. Snyder and D. L. Bish, 'Quantitative analysis' in: [12], p. 101–144.
47 D. E. Anderson and W. J. Thomson, Ind. Eng. Chem. Res., 26 (1987) 1628.
48 N. Eisenreich and W. Engel, J. Appl. Crystallogr., 16 (1983) 259.
49 W. Engel and N. Eisenreich, Thermochim. Acta, 83 (1985) 161.
50 N. Eisenreich and W. Engel, J. Thermal Anal., 35 (1989) 577.
51 S. Matsumoto, Bull. Chem. Soc. Jpn., 40 (1967) 743.
52 V. Petricek, I. Cisarova, L. Hummel, J. Kroupa and B. Brezina, Acta Crystallogr. Sect. B: Struct. Sci., 46 (1990) 830.
53 N. Gérard and G. Watelle-Marion, Bull. Soc. Chim. Fr., (1963) 2631.
54 R. Hocart, N. Gérard and G. Watelle-Marion, C. R. Acad. Sci. Paris, t.258 (1964) 3709.
55 N. Gérard and G. Watelle-Marion, C. R. Acad. Sci. Paris, t.261 (1965) 2363.
56 N. Gérard, G. Watelle-Marion and A. Thrierr-Sorel, Bull. Soc. Chim. Fr., (1967) 1788.
57 N. Gérard, J. C. Mutin and G. Watelle-Marion, C. R. Acad. Sci. Paris, t.265 (1967) 1436.
58 P. Barret, N. Gérard and G. Watelle-Marion, Bull. Soc. Chim. Fr., (1968) 3172.
59 N. Gérard, M. Lallement and G. Watelle-Marion, C. R. Acad. Sci. Paris, t.267 (1968) 1679.
60 N. Gérard, G. Watelle-Marion and A. Thrierr-Sorel, Bull. Soc. Chim. Fr., (1968) 4367.
61 N. Gérard and G. Watelle-Marion, Bull. Soc. Chim. Fr., (1969) 58.
62 N. Gérard and R. Pernolet, J. Phys. E: Sci. Instrum., 6 (1973) 512.
63 N. Gérard and R. Pernolet, 'A study of the process of formation of ethylene and ethane clathrate hydrates by thermogravimetry and X-ray diffraction', Proc. 4th Int. Symp. Fresh Water Sea, 1973, Vol.3, p. 453–460.
64 N. Gérard, J. Phys. E: Sci. Instrum., 7 (1974) 509.
65 H. Wang, D. X. Li and W. J. Thomson, J. Am. Ceram. Soc., 71 (1988) C463.
66 W. J. Thomson, 'Dynamic X-ray diffraction: a technique for following solid state reactions' in: Ceramic Transactions (W. S. Young, G. L. McVay, G. E. Pike, Eds.), Vol.5, American Ceramic Society, Westerville, Ohio, 1989, p.131–140.
67 W. J. Thomson, H. Wang, D. B. Parkman, D. X. Li, M. Strasik, T. S. Luhman, C. Han and I. A. Aksay, J. Am. Ceram. Soc., 72 (1989) 1977.
68 H. K. Cammenga, M. Epple, A. Blaschette and M. Näveke, Thermochim. Acta, 151 (1989) 171.

69 H. K. Cammenga, M. Epple and B. Baumgartner, J. Chim. Phys. Phys. Chim. Biol., 87 (1990) 1249.
70 M. Epple and H. K. Cammenga, Solid State Ionics, 63–65 (1993) 307.
71 O. Chaix-Pluchery, J. C. Niepce and D. Freund, React. Solids, 8 (1990) 323.
72 M. Näveke, P. G. Jones, A. Blaschette, D. Schomburg, H. K. Cammenga and M. Epple, Z. Anorg. Allg. Chem., 619 (1993) 1027.
73 E. Koch, J. Thermal Anal., 33 (1988) 1259.
74 A. J. Kassman, Thermochim. Acta, 84 (1985) 89.
75 G. Dénès, J. Solid State Chem., 37 (1981) 16.
76 J. Lauterjung and G. Will, Physica B (Amsterdam), 139/140 (1986) 343.
77 Ö. Sävborg, J. R. Schoonover, S. H. Lin and L. Eyring, J. Solid State Chem., 68 (1987) 214.
78 P. Hernandez, F. Lamelas, R. Clarke, P. Dimon, E. B. Sirota and S. K. Sinha, Phys. Rev. Lett., 59 (1987) 1220.
79 W. Minor, B. Schönfeld, B. Lebech, B. Buras and W. Dmowski, J. Mater. Sci., 22 (1987) 4144.
80 T. W. Little and H. Chen, J. Appl. Phys., 63 (1988) 1182.
81 J. R. Schoonover and S. H. Lin, J. Solid State Chem., 76 (1988) 143.
82 W. J. Thomson, K. A. Helling and R. J. Rodriguez, Energy Fuels, 2 (1988) 9.
83 J. Plévert, J. P. Auffrédic, M. Louër and D. Louër, J. Mater. Sci., 24 (1989) 1913.
84 D. X. Li and W. J. Thomson, J. Am. Ceram. Soc., 73 (1990) 964.
85 D. X. Li and W. J. Thomson, J. Mater. Res., 5 (1990) 1963.
86 J. P. Auffrédic, J. Plévert and D. Louër, J. Thermal Anal., 37 (1991) 1727.
87 H. Jung and W. J. Thomson, J. Catal., 128 (1991) 218.
88 L. Fister and D. C. Johnson, J. Am. Chem. Soc., 114 (1992) 4639.
89 V. Kolarik, M. Juez-Lorenzo, N. Eisenreich and W. Engel, J. Thermal Anal., 38 (1992) 649.
90 Y. Wang, D. X. Li and W. J. Thomson, J. Mater. Sci., 8 (1993) 195.
91 J. Wong, E. M. Larson, J. B. Holt, P. A. Waide, B. Rupp and R. Frahm, Science (Washington, D. C., 1883-), 249 (1990) 1406.
92 E. M. Larson, P. A. Waide and J. Wong, Rev. Sci. Instrum., 62 (1991) 53.
93 R. Frahm, J. Wong, J. B. Holt, E. M. Larson, B. Rupp and P. A. Waide, Phys. Rev. B. Condens. Matter, 46 (1992) 9205.
94 G. S. Pawley, Faraday Disc. Chem. Soc., 69 (1980) 157.
95 G. Ungar and J. L. Feijoo, Mol. Cryst. Liq. Cryst., 180B (1990) 281.
96 R. Schlögl, Angew. Chem., 32 (1993) 403; Angew. Chem. Int. Ed. Engl., 32 (1993) 381.
97 J. M. Thomas, J. Chem. Soc., Dalton Trans., (1991) 555.
98 J. W. Couves, J. M. Thomas, D. Waller, R. H. Jones, A. J. Dent, G. E. Derbyshire and G. N. Greaves, Nature (London), 354 (1991) 465.
99 P. A. Wright, S. Natarajan, J. M. Thomas and P. L. Gai-Boyes, Chem. Mater., 4 (1992) 1053.
100 H. Jung and W. J. Thomson, J. Catal., 134 (1992) 654.
101 H. Jung and W. J. Thomson, J. Catal., 139 (1993) 375.
102 R. M. Nix, T. Rayment, R. M. Lambert, J. R. Jennings and G. Owen, J. Catal., 106 (1987) 216.
103 A. P. Walker, T. Rayment and R. M. Lambert, J. Catal., 117 (1989) 102.
104 R. H. Jones, A. T. Ashcroft, D. Waller, A. K. Cheetham and J. M. Thomas, Catal. Lett., 8 (1991) 169.

105 T. G. Fawcett, C. E. Crowder, L. F. Whiting, J. C. Ton, W. F. Scott, R. A. Newman, W. C. Harris, F. J. Knoll and V. J. Caldecourt, Adv. X-ray Anal., 28 (1985) 227.
106 R. Gehrke, Top. Curr. Chem., 151 (1989) 111.
107 J. Koberstein and T. P. Russell, Macromolecules, 19 (1986) 714.
108 T. P. Russell and J. T. Koberstein, J. Polym. Sci., Part B: Polym. Phys., 23 (1985) 1109.
109 J. Barrington Leigh and G. Rosenbaum, Annu. Rev. Biophys. Bioeng., 5 (1976) 239.
110 H. D. Bartunik, Rev. Phys. Appl., 19 (1984) 671.
111 M. Caffrey, Annu. Rev. Biophys. Biophys. Chem., 18 (1989) 159.
112 K. Lohner, Chem. Phys. Lipids, 57 (1991) 341.
113 M. Caffrey, TrAc, Trends Anal. Chem. Pers. Ed., 10 (1991) 156.
114 D. W. J. Cruickshank, J. R. Helliwell and L. N. Johnson (Eds.), 'Time-resolved macromolecular crystallography', Oxford University Press, Oxford, 1992.
115 Y. Inoko and T. Mitsui, J. Phys. Soc. Jpn, 6 (1978) 1918.
116 M. J. Ruocco and G. G. Shipley, Biochim. Biophys. Acta, 691 (1982) 309.
117 M. Caffrey and D. H. Bilderback, Biophys. J., 45 (1984) 627.
118 M. Caffrey and F. S. Hing, Biophys. J., 51 (1987) 37.
119 R. D. Koynova, B. G. Tenchov, P. J. Quinn and P. Laggner, Chem. Phys. Lipids, 48 (1988) 205–214.
120 M. Caffrey, G. Fanger, R. L. Magin and J. Zhang, Biophys. J., 58 (1990) 677.
121 P. Laggner, M. Kriechbaum, G. Rapp and J. Hendrix, 'Structural pathways and short-lived intermediates in phospholipid phase transitions. Millisecond synchrotron X-ray studies', Proc. 2nd European Conference on Progress in X-ray Synchrotron Radiation Research (A. Balerna, E. Bernieri, S. Mobilio, Eds.), Bologna, 1990, SIF.
122 P. Laggner, M. Kriechbaum and G. Rapp, J. Appl. Crystallogr., 24 (1991) 836.
123 P. Laggner, Top. Curr. Chem., 145 (1988) 173.
124 P. Laggner, M. Kriechbaum, A. Hermetter, F. Paltauf, J. Hendrix and G. Rapp, Progr. Coll. Polym. Sci., 79 (1989) 33.
125 M. Kriechbaum, P. Laggner and G. Rapp, Nucl. Instrum. Meth. Phys. Res. Sect. A, 291 (1990) 41.
126 H. Chung and M. Caffrey, Biophys. J., 63 (1992) 438.
127 K. Wefers, Ber. Dtsch., Keram. Ges., 42 (1965) 35.
128 A. F. Bessonov, V. M. Ust'yantsev and G. A. Taksis, Poroshk. Metall (Kiev), 7 (1967) 92; Sov. Powder Metall. Met. Ceram. Engl. Transl., 7 (1967) 238.
129 G. B. Ravich, V. Z. Kolodyazhnyi, V. G. Brodov, A. M. Kuchomov and A. L. Zhemarkin, Russ. J. Inorg. Chem., 12 (1967) 1190.
130 H. G. Wiedemann, Thermochim. Acta, 7 (1973) 131.
131 T. G. Fawcett, E. J. Martin, C. E. Crowder, P. J. Kincaid, A. J. Strandjord, J. A. Blazy, D. N. Armentrout and R. A. Newman, Adv. X-ray Anal., 29 (1986) 323.
132 J. Y. Andersson, J. De Pablo and M. Azoulay, Thermochim. Acta, 91 (1985) 223.
133 J. Y. Andersson and M. Azoulay, J. Chem. Soc., Dalton Trans., (1986) 469.
134 R. Frahm, Nucl. Instrum. Meth. Phys. Res. Sect. A, 270 (1988) 578.
135 P. Lagarde, M. Lemonnier and H. Dexpert, Physical B (Amsterdam), 158 (1989) 337.
136 D. Bazin, H. Dexpert and P. Lagarde, Top. Curr. Chem., 145 (1988) 69.
137 D. Bazin, H. Dexpert, N. S. Guyot-Sionnest, J. P. Bournonville and J. Lynch, J. Chim. Phys. Phys. Chim. Biol., 86 (1989) 1707.
138 E. Dartyge, A. Fontaine, A. Jucha, H. Tolentino and G. Tourillon, J. Chim. Phys. Phys. Chim. Biol., 86 (1989) 1793.

139 A. Fontaine, E. Dartyge, J. P. Itié, A. Jucha, A. Polian, H. Tolentino and G. Tourillon, Top. Curr. Chem., 151 (1989) 179.
140 A. Fontaine, F. Baudelet, E. Dartyge, D. Guay, J. P. Itié, A. Polian, H. Tolentino and G. Tourillon, Rev. Sci. Instrum., 63 (1992) 960.
141 H. Tolentino, F. Baudelet, A. Fontaine, T. Gourieux, G. Krill, J. Y. Henry and J. Rossat-Mignod, Physica C (Amsterdam), 192 (1992) 115.
142 S. J. Andrews, M. Z. Papiz, R. McMeeking, A. J. Blake, B. M. Lowe, K. R. Franklin, J. R. Helliwell and M. M. Harding, Acta Crystallogr. Sect. B: Struct. Sci., 44 (1988) 73.
143 W. Rieck, H. Schulz and W. Siedel, J. Phys. Chem. Solid, 52 (1991) 1289.
144 B. C. Larson, C. W. White, T. S. Noggle and D. Mills, Phys. Rev. Lett., 48 (1982) 337.
145 D. M. Mills, B. C. Larson, C. W. White and T. S. Noggle, Nucl. Instrum. Meth. Phys. Res., 208 (1983) 511.
146 B. C. Larson, J. Z. Tischler and D. M. Mills, J. Mater. Res., 1 (1986) 144.
147 N. C. Woolsey, J. S. Wark and D. Riley, J. Appl. Cryst., 23 (1990) 441.
148 K. Kjaer, J. Als-Nielsen, C. A. Helm, L. A. Laxhuber and H. Möhwald, Phys. Rev. Lett., 58 (1987) 2224.
149 A. J. Ryan, J. Thermal Anal., 40 (1993) 887.
150 M. Bark, H. G. Zachmann, Acta Polymer., 44 (1993) 259.

Zusammenfassung — Grundlagen und Anwendungsmöglichkeiten zeit- und/oder temperature aufgelöster Beugungsmethoden werden vorgestellt. Dabei wird auf Röntgen- und Neutronenbeugung eingegangen. Dynamische Beugungsmethoden werden zunehmend in verschiedenen Bereichen wie der Festkörperreaktionskinetik, der heterogenen Katalyse und den Biowissenschaften eingesetzt. Der Einsatz neuer Methoden wie der Synchrotronstrahlung und der Ortsempfindlichen Detektoren erlaubt eine erhebliche Erweiterung der Anwendungsgebiete. An ausgewählten Beispielen werden Einsatzmöglichkeiten demonstriert. Die dynamischen Beugungsmethoden werden mit den klassischen thermoanalytischen Techniken Thermogravimetrie und DSC verglichen.